THE CLOËTTA PRIZE 2023
IS AWARDED TO

PROFESSOR

CHRISTOPH HESS

BORN IN 1970 IN ZURICH, SWITZERLAND

PROFESSOR AND HEAD OF INTERNAL MEDICINE OF THE MEDICAL OUTPATIENT DIVISION, CLINICAL IMMUNOLOGY SERVICE, UNIVERSITY HOSPITAL BASEL, IMMUNOBIOLOGY LABORATORY AT THE DEPARTMENT OF BIOMEDICINE, UNIVERSITY OF BASEL AND SENIOR FACULTY AND PRINCIPAL INVESTIGATOR, ACADEMIC HEAD CLINICAL IMMUNOLOGY IN THE DEPARTMENT OF MEDICINE AT THE UNIVERSITY OF CAMBRIDGE

FOR HIS OUTSTANDING CONTRIBUTIONS TO BIOMEDICAL RESEARCH, ESPECIALLY IN THE FIELD OF IMMUNOMETABOLISM, AND FOR HIS INTEGRATION OF BASIC FINDINGS WITH CLINICAL HUMAN IMMUNOLOGY

BASEL, 24TH NOVEMBER 2023

IN THE NAME OF THE FOUNDATION BOARD:

THE PRESIDENT

THE VICE PRESIDENT

A MEMBER

CHRISTOPH HESS

CURRICULUM VITAE

Personal Information

Family and first name:	Hess-Umbricht Christoph
Place of birth:	Zürich, Switzerland
ORCID:	0000-0003-0364-8825

Job address and contact details:
Medical Outpatient Division | Clinical Immunology Service | Immunobiology Laboratory | University and University Hospital Basel | 20 Hebelstrasse | 4031 Basel | Switzerland

Department of Medicine | Cambridge Institute of Therapeutic Immunology & Infectious Disease | Jeffrey Cheah Biomedical Centre | University of Cambridge | Puddicombe Way | Cambridge CB2 0AW | UK

voice: +41 (0) 61 265 44 75 (CH)
email: ch818@cam.ac.uk; chess@uhbs.ch

Education and employment history

1990–1996	Medical school Zurich and Lausanne & USMLE 1&2
1997–1999	MD PhD training, University of Basel
2000–2001	Clinical training: Internal Medicine, University Hospital Basel, BS
2001–2001	Clinical training: Imperial College, Hammersmith Hospital, London, UK
2002–2004	Fellowship, Massachusetts General Hospital/Harvard Medical School, USA
2004–2007	SCORE Fellow and specialist Registrar, University Hospital BS
2005	Junior faculty position, University of Basel
2007–6/2009	SNSF Professorship grant, University Hospital BS
2006	Diploma *Internal Medicine* (FMH)
2006	Diploma *Consultant Immunologist* (DGfI)

2007–2009	Consultant, Internal Medicine, University Hospital BS
Since 7/2009	Senior Faculty and Head, Internal Medicine, Outpatients, University Hospital BS
Since 2012	Lead – Clinical Immunology (primary immunodeficiency and autoimmunity)
Since 4/2019	Senior Faculty and Principal Investigator, Academic Head Clinical Immunology, University of Cambridge, Department of Medicine, UK (dual affiliation with University of Basel).

Approved research projects

Current only (PI unless stated otherwise)		
Wellcome Trust, 2020 (4 Co-PIs)	GBP	4.041.000
SNSF project grant, 2021	CHF	1.224.000
BBSRC PhD studentship grant, 2019	GBP	102.000
SNSF project grant, 2022	CHF	904.000
Uniscientia Foundation grant, 2021	CHF	298.000
Milner Consortium grant, 2022	GBP	950.000
NSMBF Project grant, 2023	CHF	80.000
BSI/CRUK Prime Funding, 2023	GBP	25.000

Teaching activities

Internal Medicine; Immunology – Faculty of Medicine, Basel University
Translational Medicine and Immunology – Faculty of Science, Basel University
Supervision of Masters-, MD-, MD-PhD- and PhD-students

Clinical activities

Outpatient: evaluation/treatment of patients with complex systemic autoimmune disorders and primary immune dysregulation and -deficiencies.

Inpatient: evaluation/treatment of patients across the spectrum of general internal medicine. *University Center for Immunology (initiated and established jointly with Alex Navarini):* Weekly interdisciplinary patient discussions.

Panels/boards/review activity
Head, Euro-Exchange Program for Residents (2010–2018)
Swiss Transplant Cohort Study – Scientific Board, since 2006
Novartis Foundation for Medical-Biological Research, since 2015
Goldschmidt-Jacobson Foundation, University of Basel (2014–2018)
University of Basel Research Board (2015-2018)
SNSF Research Council – Division 3, since 2018
Board of Reviewing Editors, Science, since 2021
Ad hoc reviewer activity for journals (selection): Science; Cell; Nature Immunology; Nature Cell Biology; Nature Communications; Immunity; Cell Metabolism; Cell Reports; Journal of Experimental Medicine; Journal of Clinical Investigation; European Journal of Immunology; EMBO Journal; FEBS journal; Trends in Immunology
Ad hoc reviewer for granting bodies: MRC, UK; Wellcome Trust, UK; Science Foundation Ireland; German-Israel Foundation for Scientific Research and Development; Kay Kendall Leukaemia Fund, UK; Tenovus Cancer Charity, UK

Memberships
Swiss Society of Internal Medicine (FMH) – full license to practice
General Medical Council, UK (Specialist Register) – full license to practice
Swiss Society of Allergy and Immunology
Swiss Transplantation Society
German Society of Immunology
Royal College of Physicians, UK
European Society of Immunodeficiency (ESID)
American Association of Immunologists
Fellow of the Royal College of Physicians (UK)
Member of the Swiss Academy of Medical Sciences

Fellowships, prizes/awards

Fellowships
SNSF MD PhD stipend (1997–99)
SNSF Advanced Postdoc mobility fellowship (2002–2004)
SNSF SCORE fellowship (2004–2006)
SNSF Professor fellowship (2007–2011)

Research
Faculty award 2001, MD-thesis, University of Basel
Pfizer Young Investigator award 2001
Swiss Transplant award 2006, 1st Prize
Dep. of Biomedicine 2013; best publication of the year
Cloëtta price 2023

Teaching
Since 2009: 7x *excellent teacher award* (selection by medical students)

Patents
IRP-mediated improvement of cell therapy (EP19192299.6)
LFA-1 signaling mediator for use in cancer therapy (EP20/191392.8)
Compositions for the Treatment of EBV Associated Diseases
or Conditions (EP 21161105.8 and PCT/EP2022/055647)
Non-canonical PHGDH-mediated improvement of cell therapy
(EP22163501.4)

SELECTED PUBLICATIONS

Ruffieux H., A. L. Hanson, S. Lodge, N.G. Lawler, L. Whiley, N. Gray, T.H. Nolan, L. Bergamaschi, F. Mescia, L. Turner, A. de Sa, V.S. Pelly; CITIID-NIHR BioResource COVID-19 Collaboration; P. Kotagiri, N. Kingston, J.R. Bradley, E. Holmes, J. Wist, J.K. Nicholson, P.A. Lyons, K.G.C. Smith, S. Richardson, G.R. Bantug, **C. Hess.** A patient-centric characterization of systemic recovery from SARS-CoV-2 infection. Nature Immunology 2023. 24:349–358.

Loetscher J., A.-A. Martí i Líndez, N. Kirchhammer, G. Giordano, E. Cribioli, M. Trefny, M. Lenz, P. Strati, M. Künzli, P. Dehio, J. Loeliger, L. Litzler, D. Schreiner, V. Koch, D. Lee, J. Graehlert, A.-V. Burgener, M. L. Balmer, M. Irving, W. Reith, C. G. King, A. Zippelius, **C. Hess.** Extracellular Mg2+ regulates memory $CD8^+$ T cell effector maturation via LFA-1. Cell 2022. 185:585–602.e29.

Balmer M. L., R. Epple, E. H. Ma, A. Egli, L. Bubendorf, K. Rentsch, A.-K. Woischnig, N. KhannaJ. Loeliger, J. Loetscher, P. Dehio, G. Perrin, J. D. Warncke, O. P. Schären, C. M. Schürch, G. Unterstab, A. Thompson, S. Hapfelmeier, R. G. Jones, **C. Hess.** Memory $CD8^+$ T cells balance pro- and anti-inflammatory activity by reprogramming cellular acetate handling at sites of infection. Cell Metabolism 2020. 32: 457–467.

Dimeloe S., P. Gubser, J. Loeliger, C. Frick, L. Develioglu, M. Fischer, F. Marquardsen, G. R. Bantug, D. Thommen, Y. Lecoultre, A. Zippelius, A. Langenkamp, **C. Hess.** Tumor-derived TGF-β inhibits mitochondrial respiration to suppress IFN-β production by human CD4+ T cells. Science Signaling 2019. 12, 599: eaav3334.

Burgener A.-V., G. R. Bantug, B. Meyer, R. Higgins, A. Ghosh, O. Bignucolo, E. H. Ma, J. Löliger, G. Unterstab, M. Geigges, R. Steiner, M. Enamorado, R. Ivanek, D. Hunziker, A. Schmidt, B. Müller-Durovic, J. Grählert, R. Epple, S. Dimeloe, J. Lötscher, U. Sauder, M. Ebnöther, B. Burger, I. Heijnen, S. Martínez-Cano, N. Cantoni, R. Brücker, C. R. Kahlert, D. Sancho, R. G. Jones, A. Navarini, M. Recher, **C. Hess.** SDHA gain-of-function engages inflammatory mitochondrial retrograde signaling via KEAP1–Nrf2. Nature Immunology 2019. 20, 1311–1321.

Bantug G., M. Fischer, J. Grählert, M.L. Balmer, G. Unterstab, L. Develioglu, R. Steiner, L. Zhang, A.S. Henriques da Costa, P.M. Gubser, A.-V. Burgener, U. Sauder, J. Löliger, R. Belle, S. Dimeloe, J. Lötscher, A. Jauch, M. Recher, G. Hönger, M.N. Hall, P. Romero, C. Frezza, **C. Hess.** Mitochondria–ER contact sites are immunometabolic hubs that orchestrate the rapid recall response of memory $CD8^+$ T cells. Immunity 2018. 48:542–555.

Ma E.H., G. Bantug, T. Griss, M.J. Verway, R.M. Johnson, S. Condotta, T.C. Raissi, H. Tsui, B. Samborska, G. Boukhaled, M. Balmer, S. Henriques da Costa, C. Frezza, C. M. Krawczyk, M.J. Richer, **C. Hess,** R.G. Jones. Serine is an essential metabolite for effector T cell expansion. Cell Metabolism 2017. 2:345–357.

Balmer M.L., E.H. Ma, G.R. Bantug, J. Grählert, S. Pfister, T. Glatter, A. Jauch, S. Dimeloe, E. Slack, P. Dehio, M.A. Krzyzaniak, C.G. King, A.-V. Burgener, M. Fischer, L. Develioglu, R. Belle, M. Recher, W.V. Bonilla, A.J. Macpherson, S. Hapfelmeier, R.G. Jones, **C. Hess.** Memory $CD8^+$ T Cells Require Increased Concentrations of Acetate Induced by Stress for Optimal Function, Immunity 2016. 44:1312–1324.

Kolev M., S. Dimeloe, G. Le Friec, A. Navarini, G. Arbore, G.A. Povoleri, M. Fischer, R. Belle, J. Loeliger, L. Develioglu, G.R. Bantug, J. Watson, L. Couzi, B. Afzali, P. Lavender, **C. Hess*** and Claudia Kemper* (* equal contribution and corresponding author). CD46 links complement and metabolic reprogramming in human Th1 responses, Immunity 2015. 16:1033–47.

Gubser P., G.R. Bantug, L. Razik, M. Fischer, S. Dimeloe, G. Heonger, B. Durovic, A. Jauch, **C. Hess.** Rapid effector function of memory $CD8^+$ T cells requires an immediate-early glycolytic switch. Nature Immunology 2013. 14:1064–72.

METABOLIC REGULATION OF T CELL FUNCTION

Christoph Hess

Introduction

T cells are a key component of the adaptive immune system, acting as both coordinators and effectors of immunity. As such, T cells are instrumental in protecting the host from invading pathogens. The different stages of T cell activation, expansion and contraction are integrated with systemic inflammation and the control of microbial growth. However, when activated inappropriately – due to cell-intrinsic or cell-extrinsic factors – T cells contribute to a wide spectrum of diseases (1–5).

T cell metabolic reprogramming is crucial for the differentiation, proliferation and acquisition of effector functions. A key change in cellular metabolism in activated T cells is the upregulation of aerobic glycolysis (that is, the conversion of glucose-derived pyruvate into lactate under normoxic conditions). Although this is an energetically inefficient process, the engagement of aerobic glycolysis promotes the build-up of biochemical intermediates that are necessary for nucleotide, amino acid and fatty acid synthesis. Glycolytic metabolites and interlinked pathways, such as the pentose phosphate pathway and glycerol and amino acid synthesis pathways, as well as pyruvate usage, are essential for the proper functioning of activated T cells. Concomitant with changes in glucose metabolism, T cell activation also enhances mitochondrial biogenesis and oxidative phosphorylation (OXPHOS) and drives mitochondrial membrane hyper-polarization, amino acid uptake and glutaminolysis. Mitochondria, in addition to their primary role in generating ATP, play further key metabolic roles, such as in calcium buffering, the generation of reactive oxygen species (ROS), nitrogen metabolism or the fueling of cytoplasmic acetyl-CoA synthesis and lipogenesis. Each of these mitochondrial pro-

cesses is known – or is likely – to have links to T cell function. Metabolic pathway usage is subject to regulation on multiple levels, both intrinsic (for example, allosteric regulation of enzymes in a given pathway, such as inhibition of phosphofructokinase by ATP), and extrinsic in nature (for example, upregulation of glycolytic enzymes in proliferating cells receiving activating signals via stimulatory receptors). Key metabolic checkpoint kinases, such as mechanistic target of rapamycin (mTOR) and 5'-AMP-activated kinase (AMPK), integrate extrinsic signals and intracellular nutrient and energy abundance to initiate appropriate metabolic reprogramming (**Figure 1,** from (6)):

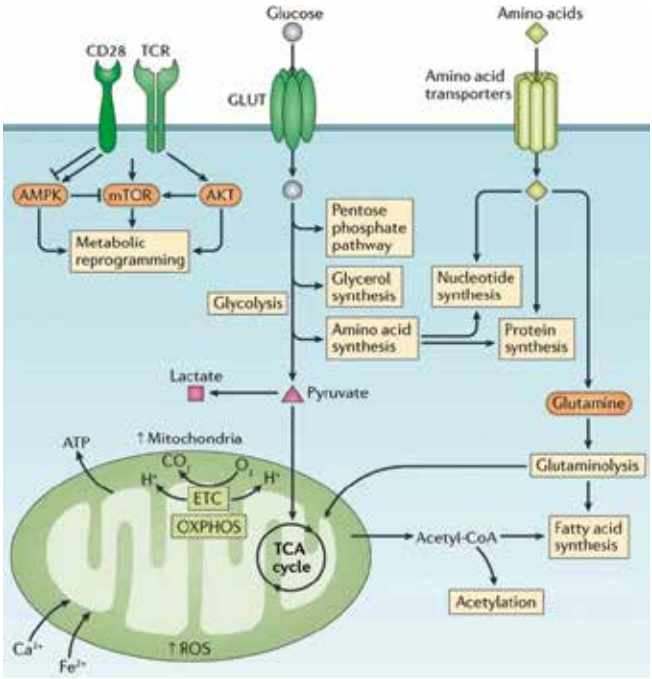

Figure 1. Metabolic changes that accompany effector T cell maturation. *Abbreviations: ETC, electron transport chain; GLUT, glucose transporter; TCA, tricarboxylic acid; TCR, T cell receptor.*

The metabolic requirements that support the pivotal rapid memory functionality have been a focus of our work. Here, I will summarize a few contributions we made over the years to the now burgeoning field of immunometabolism, covering basic, translational and clinical aspects.

Fundamental research into the metabolic regulation of T cells

Glucose and mitochondrial metabolism orchestrate effector T cell function

During acute viral infection, pathogen-specific naive $CD8^+$ T cells become activated, followed by clonal expansion and differentiation into cytotoxic effector cells (7). Resolution of infection triggers the contraction of effector cell populations, accompanied by the formation of a long-lived memory pool (8). In a highly coordinated process, memory $CD8^+$ T cells subsequently enhance host protection after secondary infection (recall response) (8).

Naive and memory $CD8^+$ T cells are metabolically quiescent cells, which depend mainly on OXPHOS as their energy source (9–11). Ligation of the T cell antigen receptor (TCR) and subsequent costimulation of quiescent cells initiates substantial changes in cellular metabolic pathway use (12). Upregulation of aerobic glycolysis (the Warburg effect) is an important feature of this metabolic adaptation and is a prerequisite for the growth and population expansion of $CD8^+$ T cells (13–15). Augmented glycolysis by proliferating cells is linked to enhanced glucose uptake and increased expression and activity of glycolytic enzymes, whereas glucose use via OXPHOS is decreased (16, 17). This 'metabolic switch' satiates higher energy demands and provides biochemical intermediates used in the biosynthesis of macromolecules (18).

The early recall phase of an immune response relies on antigen-experienced T cells that are able to acquire effector function with rapid kinetics (19). Effector memory (EM) $CD8^+$ T cells are specialized antigen-experienced lymphocytes that traffic between blood and non-lymphoid tissues (20–23). EM $CD8^+$ T cells are ideally positioned to rapidly respond and execute effector functions at sites of infection. We

found that EM CD8⁺ T cells have an immediate-early ability to take up and metabolize glucose in a sustained manner. Additionally, we demonstrated that co-stimulation via CD28 signaling was critical for sustaining the immediate-early glycolytic switch of EM CD8⁺ T cells (**Figure 2**).

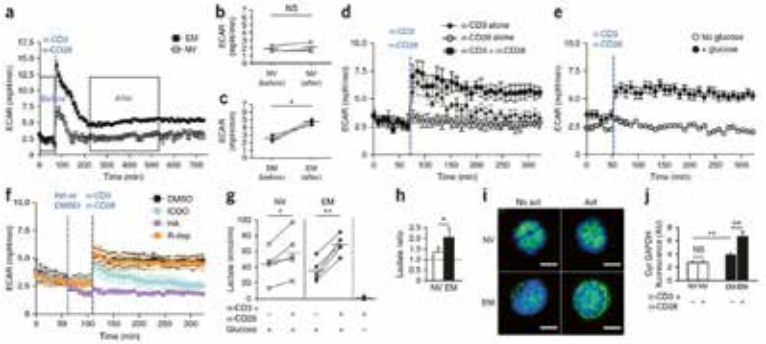

Figure 2. Memory CD8⁺ T cells are equipped with a preformed capacity to rapidly engage glycolytic activity. ***(a)*** *Extracellular acidification rate (ECAR; a measure of glycolysis) of naive and EM CD8⁺ T cells before and after 'in-Seahorse' activation with anti-CD3 (α-CD3) and anti-CD28 (α-CD28); boxes outline ECAR values used for calculation of means before and after injection.* ***(b,c)*** *Mean ECAR values before and after injection of anti-CD3 plus anti-CD28 onto plated naive CD8⁺ T cells* ***(b)*** *or EM CD8⁺ T cells* ***(c).*** ***(d)*** *ECAR of EM CD8⁺ T cells activated with anti-CD3 or anti-CD28 alone or the mAbs together (key).* ***(e)*** *ECAR of bulk CD8⁺ T cells activated with anti-CD3 and anti-CD28 in the presence of 10 mM glucose (+ glucose) or glucose-free medium (No glucose).* ***(f)*** *ECAR of bulk CD8⁺ T cells pretreated with dimethyl sulfoxide (DMSO) or the inhibitor (Inh) iodoacetate (IODO; inhibitor of the glycolytic enzyme Glyceraldehyde 3-phosphate dehydrogenase; GAPDH), heptelidic acid (HA; GAPDH inhibitor) or R-(−)-deprenyl hydrochloride (R-dep; MAO inhibitor, used as a control) before activation as in* ***e.*** ***(g)*** *Quantification of lactate in the medium of naive and EM CD8⁺ T cells (n = 5 donors) left nonactivated (−) or activated (+) with anti-CD3 plus anti-CD28 with or without glucose (bottom row).* ***(h)*** *Linear-regression analysis of the lactate concentrations in (g), presented as lactate in activated cells/lactate in nonactivated cells.* ***(i)*** *Microscopy of naive and EM CD8⁺ T cells left non-activated (No act) or activated (Act) for 2 h with anti-CD3 and anti-CD28: green, GAPDH; blue, DAPI. Scale bars, 3 μm.* ***(j)*** *Fluorescence intensity of cytoplasmic GAPDH in naive*

and EM CD8⁺ T cells left nonactivated (−) or stimulated (+) for 2 h with anti-CD3 plus anti-CD28; total cells: n = 30 (nonactivated naive), 43 (activated naive), 47 (nonactivated EM) or 70 (activated EM). Each symbol ***(b,c,g)*** *represents an individual donor; small horizontal lines indicate the mean. *P < 0.05 and **P < 0.001 (paired two-tailed Student's t-test* ***(b,c,g),*** *linear-regression analysis* ***(h)*** *or Mann-Whitney U-test* ***(j)****). Data are representative of three experiments* ***(a-d,i,j),*** *one experiment* ***(e),*** *four experiments* ***(f)*** *or five experiments* ***(g,h;*** *all one experiment per donor; mean and s.e.m. in* ***a,d-f,h,j).***

The rapid production of IFN-γ by EM naive CD8⁺ T cells but not by naive CD8⁺ T cells suggested differences in epigenetic regulation of the *IFNG* promoter. Increased glycolytic activity in proliferating cells decreases the cellular ratio of NAD^+ to NADH, which can affect epigenetic modifications, such as deacetylation mediated by NAD^+-sensitive class III histone deacetylases (17, 24). To determine the effect of immediate-early glycolysis on NAD^+/NADH, we assessed the concentration of NAD^+ and NADH in unstimulated EM CD8⁺ T cells and those activated with anti-CD3 plus anti-CD28. At 6 h after activation, there was only a small yet significant increase in NAD^+ concentration in EM CD8⁺ T cells **(Figure 2a).** Notably, NADH concentrations were very low or undetectable under nonactivating and immediate-early–activating conditions **(Figure 3a).** We detected substantial changes in the total NADH concentration and in NAD^+/NADH only in actively proliferating CD8⁺ T cells **(Figure 2a)** and in proliferating Jurkat human T lymphocytes (data not shown). Despite the small increase in NAD^+ early after activation, EM CD8⁺ T cells rapidly produced IFN-γ in a glycolysis-dependent manner (data not shown). Hence, the small increase in NAD^+ did not seem to have a functionally relevant effect on *IFNG* transcription. These findings also demonstrated that NAD^+/NADH in resting and nascently activated EM CD8⁺ T cells favored NAD^+, which emphasized a difference in the bioenergetic status of immediate-early activated CD8⁺ T cells and that of proliferating CD8⁺ T cells.

Histones are modified differently in the *IFNG* promoter in naive versus memory CD8⁺ T cells (25). Specifically, hyperacetylation of histone H3 Lys9 (H3K9) in the *IFNG* promoter of memory CD8⁺ T cells reflects an active chromatin conformation state (25). Additionally, in mouse CD8⁺ T cells, substantial chromatin remodeling (i.e., histone loss) takes place

in the promoters of *Gzmb* (which encodes granzyme B) and *Ifng* after activation, which facilitates binding of RNA polymerase II and gene expression (26, 27). It is well established that glycolysis provides substrates for histone acetylation (28); however, its effect on chromatin remodeling remains undefined. To determine the effect of immediate-early glycolysis on histone loss and modification in the *IFNG* promoter of nascently activated memory $CD8^+$ T cells, we assessed total histone H3 and acetylated H3K9 in proximal and distal regions of the promoter (positions -7, -382 and -4179 relative to the transcription start site) after activation. We observed a substantial loss of histone H3, indicative of rapid chromatin remodeling, in all three regions of the *IFNG* promoter in both naive and EM $CD8^+$ T cells after 6 h of stimulation with anti-CD3 plus anti-CD28 **(Figure 3b).** In the presence of 2-DG, loss of histone H3 at the *IFNG* promoter was abrogated in activated EM $CD8^+$ T cells **(Figure 3b),** which indicated a role for immediate-early glycolysis in chromatin remodeling. Under non-activating conditions, there was a greater abundance of acetylated H3K9 in all three *IFNG* promoter regions in EM $CD8^+$ T cells than in naive $CD8^+$ T cells **(Figure 3b),** reflective of the active state of *IFNG* promoters in memory $CD8^+$ T cells (25).

After activation, there was a marked decrease in detectable acetylated H3K9 in the *IFNG* promoter of both subpopulations **(Figure 3b).** The observed loss of acetylated histone H3 was in agreement with the lower total histone H3 content at the *IFNG* promoter of activated $CD8^+$ T cells. Notably, the abundance of acetylated H3K9 remained higher in activated EM $CD8^+$ T cells than in their activated naive counterparts **(Figure 2b),** which indicated that the IFNG promoter of activated EM $CD8^+$ T cells maintained an active chromatin conformation state. Finally, similar to the effect of 2-DG on histone H3 content, the abundance of acetylated H3K9 in EM $CD8^+$ T cells activated in the presence of 2-DG was similar to that of nonactivated control cells **(Figure 3b),** which again indicated the importance of immediate-early glycolysis in regulating the positioning of histone H3 in the *IFNG* promoter of activated memory $CD8^+$ T cells. Together these findings established that the diminished IFN-γ synthesis in EM $CD8^+$ T cells after blockade of immediate-early glycolysis was linked to the abrogation of chromatin remodeling in the *IFNG* promoter region and not to lower abundance of acetylated H3K9.

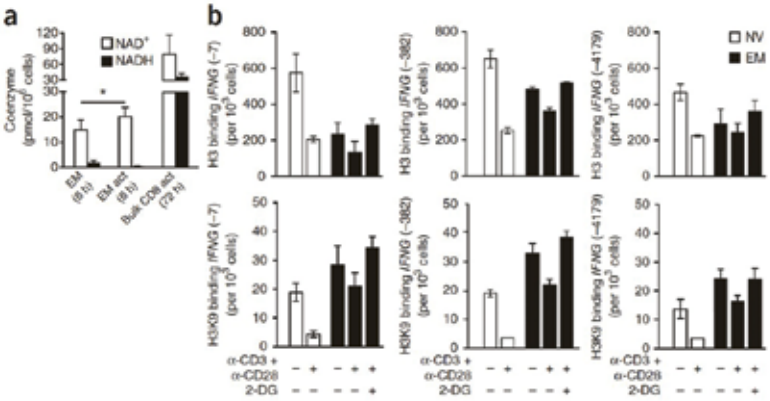

Figure 3. Metabolism interlinks with epigenetic remodeling in activated memory CD8⁺ T cells. ***(a)*** *NAD⁺ and NADH in EM CD8⁺ T cells (n = 5 donors) cultured for 6 h under nonstimulating conditions (left) or stimulated with anti-CD3 plus anti-CD28 (middle) or in bulk CD8⁺ T cells activated for 72 h (right). *P < 0.05 (paired two-tailed Student's t-test).* ***(b)*** *Chromatin-immunoprecipitation analysis of naive and EM CD8⁺ T cells left unstimulated or activated for 6 h with anti-CD3 plus anti-CD28 in the presence or absence of 2-DG, assessing the binding of histone H3 (top) or acetylated H3K9 (bottom) to the various regions of the IFNG promoter (vertical axes). Data are representative of five experiments (**a;** one donor per experiment; error bars, s.e.m.) or one experiment with cells pooled from three donors (**b;** error bars, s.d.).*

Together these data identified CD8⁺ memory T cells to have an 'imprinted' glycolytic potential required for efficient immediate-early IFN-γ recall responses. Conceptually the report was the first to link environmental signals, metabolic reprogramming and epigenetic adaptation in T cells (29).

We then interrogated the molecular and subcellular structural elements enabling enhanced glucose metabolism in nascent activated memory CD8⁺ T cells, and the molecular metabolic link between glycolysis and epigenetic remodeling. Glucose metabolism is tightly interlinked with mitochondrial function. How mitochondrial respiration in memory CD8⁺ T cells is altered early following activation remained largely un-

explored. Thus, we first examined respiration in non-activated versus nascent activated naive and EM human $CD8^+$ T cells, *in vitro*. As previously demonstrated, both maximal and spare respiratory capacities were greater in EM than in naive $CD8^+$ T cells under non-activated conditions **(Figure 4a)** Following activation, a noticeable increase in mitochondrial respiration was observed in activated EM $CD8^+$ T cells but not in naive counterparts **(Figure 4a).** Glycolysis was elevated in both activated $CD8^+$ T cell subsets, with EM cells displaying, as expected, a more prominent increase than naive cells (29).

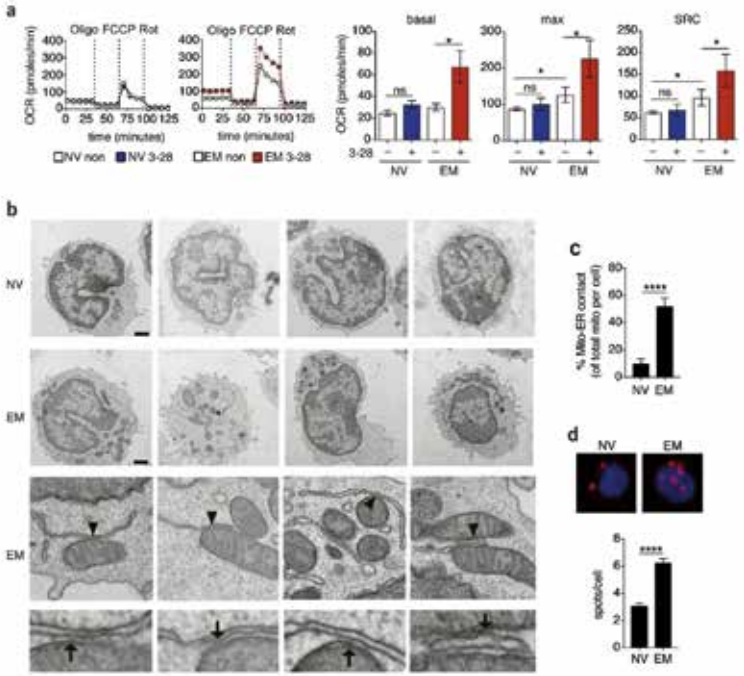

Figure 4. Effector memory CD8⁺ T cells selectively increase respiration upon activation and possess abundant mitochondria-associated ER membranes. ***(a)*** *Left, representative mitochondrial perturbation assays of naive (NV) and EM human CD8⁺ T cells left non-activated (non) or activated for 12 h with plate-bound α-CD3 and soluble α-CD28 mAb (3–28). Mitochondrial perturbation was performed by sequential treatment with oligomycin (Oligo), FCCP, and rotenone (Rot). Oxygen consumption rate (OCR) was measured by metabolic flux analysis. Right, summary bar graphs showing calculated basal respiration, maximal respiration (max), and spare respiratory capacity (SRC) in non-activated (–) or activated (+) NV and EM human CD8⁺ T cells.* ***(b)*** *Transmission electron microscopy images of NV (top) and EM (middle and bottom) human CD8⁺ T cells. Arrowheads mark mitochondria and ER contact sites that were digitally magnified in the bottom panel. Arrows show electron-dense regions of mitochondria-ER junctions. Scale bars, 1,000 nm.* ***(c)*** *Percentage of mitochondria-ER contact sites per cell in NV and EM human CD8⁺ T cells.* ***(d)*** *Top, representative proximity ligation assay (PLA) images of freshly sorted NV (left) and EM (right) human CD8⁺ T cells probed with*

*α-IP3R1 and α-VDAC1 antibodies. Red spots indicate contact sites between mitochondria (α-VDAC) and ER (α-IP3R). Cells were counterstained with DAPI (blue). Bottom, quantitative analysis of PLA from 3 donors. Data are presented as mean ± s.e.m. Two-tailed paired Wilcoxon signed rank tests (a) and two-tailed unpaired Student's t test (c and d) were used to compare groups. *P < 0.05, ****P < 0.0001, ns, not significant.*

Mitochondria-ER interactions have been shown to modulate mitochondrial respiration and bioenergetics in non-immune cells (30), although the molecular composition of mitochondria-ER tethering complexes in metazoans is not fully defined (31). In search of additional ultra-structural features that may offer a biologic basis for the contrasting activation-induced respiration phenotypes of naive versus EM $CD8^+$ T cells, we evaluated the abundance of mitochondria-ER contact sites in both subsets. We observed that in naive cells, mitochondria in close association to the ER were sparse (**Figure 4b,** top panel, and **Figure 4c**). In EM cells, by contrast, the frequency of mitochondria-ER contacts per cell was higher (**Figure 4b,** middle panels, and **Figure 4c**). The average distance between apposed ER and mitochondrial membranes in EM $CD8^+$ T cells was 21 nm (data not shown). Electron-dense zones between the mitochondrial outer membrane and ER at contact sites indicated that these organellar appositions were distinct subcellular structures (**Figure 4b,** bottom panel). To further elaborate on these findings, we performed proximity ligation assays (PLA) to quantify the abundance of mitochondria-ER junctions in naive and EM $CD8^+$ T cell subsets. Mitochondria-ER contacts were detected and enumerated by using α-VDAC1 (mitochondria) and α-IP3R1 (inositol triphosphate receptor 1, ER) antibodies as probes (32). Once again, the abundance of mitochondria-ER contact sites was found to be lower in naive cells compared to EM $CD8^+$ T cells **(Figure 4d).** In all, these data identified (a) a rapid increase in mitochondrial respiration as a distinct functional feature of EM $CD8^+$ T cells and (b) increased abundance of mitochondrial-ER contacts as a defining structural characteristic of EM $CD8^+$ T cells.

Downstream interrogation of the functional relevance and molecular composition of mitochondrial-ER contacts demonstrated that:

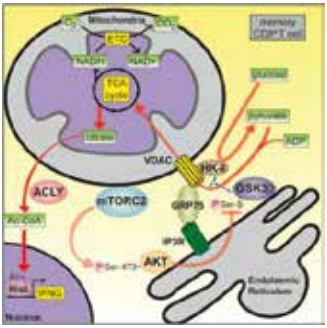

(i) mitochondrial respiration in newly activated memory T cells was intricately tied to their physical association with the ER
(ii) stable mitochondria-ER contacts support mTORC2-Akt-GSK3β signaling, which in turn allows recruitment of HK-I to mitochondria.
(iii) HK-I binding to VDAC in memory CD8⁺ T cells altered VDAC conductance, enabling metabolism of glucose-derived pyruvate in the mitochondria
(iv) pyruvate-derived citrate was key for generating acetyl-CoA by ACLY and subsequent histone acetylation ***(Figure 5)*** *from (33).*

Figure 5. Graphical summary of the structural and molecular underpinnings enabling rapid CD8+ T cell effector function.

Integration of organismal- and T cell intrinsic metabolism

Whether acutely altered organismal metabolism during acute infections impacts immune cell function by altering cell-intrinsic metabolism has not been explored. Systemic acetate release occurs in catabolic and metabolic stress conditions (34). Pathogen invasion triggers a series of defined innate defensive mechanisms and concurrent systemic catabolic metabolism (35). The hypothesis that catabolism *per se,* and the consequent availability of free acetate, might serve a specific function for host resistance to infection has not been experimentally explored. We found that acetate accumulates in the serum within hours of systemic bacterial infections **(Figure 6).**

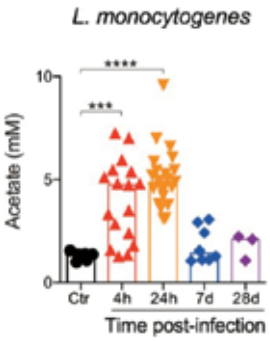

Figure 6. Acetate is an acute-phase metabolite. *Serum acetate concentrations following i.v. infection with 5,000 CFU Listeria monocytogenes. Each dot represents one mouse, bars indicate means of pooled data. One-way ANOVA was used to compare groups. ***P < 0.001, ****P < 0.0001.*

We thus went on and tested how raising acetate-levels from homeostatic to stress levels affected production of IFN-γ and interlinked glycolytic capacity in memory $CD8^+$ T cells. A notable increase in both glycolytic reserve and production of IFN-γ was observed in these experiments **(Figure 7).**

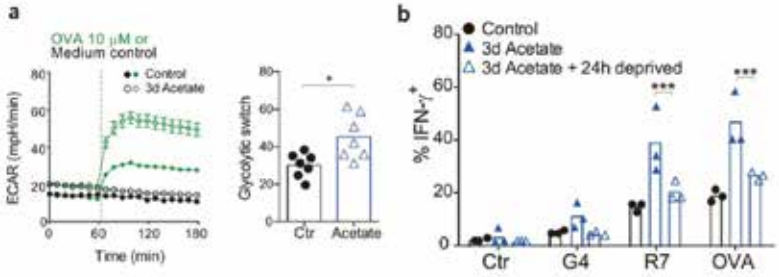

Figure 7. Acetate regulates glycolysis and interlinked effector function of memory CD8⁺ T cells. (a) *Left panel: Representative ECAR-measurements of control (filled symbols) and 3-day acetate-exposed (open-symbols) OT-I memory T cells, after injection of medium control (black) or OVA peptide (green) directly into metabolic flux analyzer (dashed line). Right panel: Glycolytic switch (mpH/min) was calculated by subtracting maximal ECAR from baseline ECAR-measurements in control (black dots) and 3 day acetate-exposed (blue triangles) OT-I memory T cells.* ***(b)*** *Percentage of IFN-γ positive OT-I memory T cells 4 h after re-stimulation with medium control (Ctr), or the APLs G4 and R7, or OVA peptide, determined by ICS. Cells were cultured in control medium (black dots) or acetate medium (5 mM) (filled blue triangles) for 3 days, and then switched back to control medium (open blue triangles) for 24 h. Each dot represents data obtained from cells isolated from one mouse, and bars indicate means of pooled data. Unpaired t test (a) and two-way ANOVA (b) were used to compare groups. *P < 0.05, ***P < 0.001.*

To gain a more detailed understanding of acetate metabolism in OT-I memory T cells, we performed tracing studies. These experiments showed that acetate contributed substantially to citrate and acetyl-CoA production and suggested the conversion of citrate to acetyl-CoA by ATP citrate lyase (ACLY). Inhibiting ACLY in OT-I memory T cells during acetate exposure using two different inhibitors blocked the acetate-mediated augmentation of IFN-γ production. In line with this, knockdown of *Acly* also reduced the capacity of OT-I cells to produce IFN-γ. Together these data indicated that acetyl-CoA, derived from the enzymatic conversion of citrate by ACLY, was key in mediating acetate-induced enhancement of memory T cell function (data not shown). In addition to co-regulating gene transcription via acetylation of histones, acetylation of most of the enzymes of the glycolytic pathway and the TCA cycle has been shown to occur, influencing enzymatic

activities via several proposed mechanisms (36). Glyceraldehyde 3-phosphate dehydrogenase (GAPDH) is among the most abundantly expressed glycolytic enzymes across multiple tissues and a rate-limiting step of aerobic glycolysis (37, 38). In memory T cells, GAPDH regulates rapid IFN-γ production – as discussed above (29). We therefore aimed to assess whether GAPDH played a role in linking the increased cellular acetyl-CoA pool and IFN-γ production after acetate exposure. First, expression of GAPDH was re-assessed both at the mRNA and the protein level in OT-I memory T cells cultured for 3 days in acetate versus controls and confirmed to be similar **(Figure 8a).** Next we explored the possibility that exogenous acetate exerted a regulatory function on OT-I memory T cells by acetylation of GAPDH, thus increasing its catalytic activity (36, 39) Indeed, GAPDH functional activity was significantly increased in acetate-exposed cells **(Figure 8b).** This gain of function was not observed when garcinol, an inhibitor of acetyltransferases (40), was added to the cell culture during acetate exposure **(Figure 8b).** Lysates of acetate-exposed and acetate-deprived OT-I memory T cells were next probed by Western blot, using an acetylated-lysine-specific antibody. The most prominent band detected in OT-I memory T cells after 3 days of exposure to acetate was at the size of GAPDH (37 kDa) **(Figure 8c).** To formally test whether exposure of OT-I memory T cells to acetate resulted in acetylation of GAPDH, we analyzed immunoprecipitated GAPDH by mass-spectrometry. GAPDH was acetylated at lysine K217, a previously described acetylation site of murine GAPDH (41), in acetate-exposed OT-I memory T cells, but not in control cells **(Figure 8d).** In order to directly define the functional importance of acetylation at K217 for GAPDH function, we investigated enzymatic activity of GAPDH mutated at K217 (K→A). Despite providing non-limiting amounts of glucose and acetate, GAPDH functional activity was significantly lower in fibroblasts transfected with the GAPDH K217 mutant **(Figure 8e).** This reduced activity was also recapitulated in metabolic flux studies (data not shown). The requirement for acetylation to support GAPDH enzymatic activity was confirmed by deacetylation assays, using the bacterial de-acetylase CobB **(Figure 8e).**

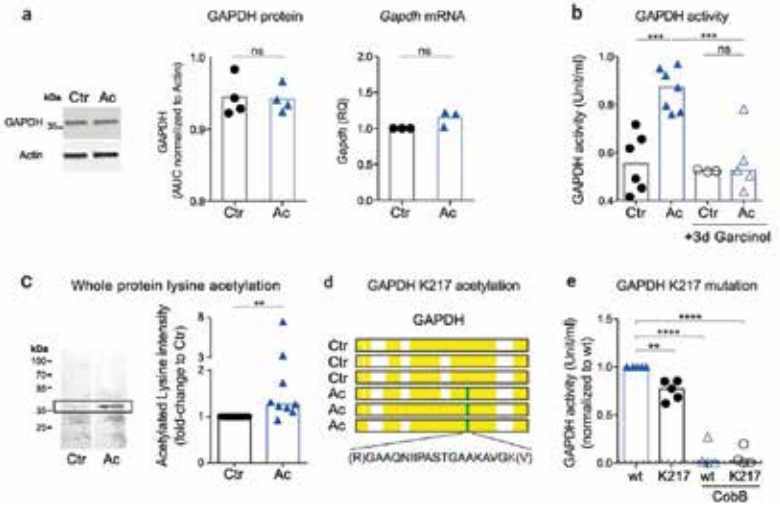

Figure 8. Acetylation of GAPDH regulates the enzymatic activity. ***(a)*** *Representative Western blot from whole-protein extracts of control (Ctr, black dots) and 3 day acetate-exposed (Ac, blue triangles) OT-I memory T cells, probed for GAPDH and Actin. GAPDH protein concentration was quantified and normalized to Actin (middle). Gapdh mRNA normalized to 18S and control memory cells, determined by RT PCR, are shown in the right panel.* ***(b)*** *GAPDH activity measured in cell lysates of control (Ctr, black dots) and 3-day acetate-exposed (Ac, blue triangles) OT-I memory T cells in the presence (open symbols) or absence (filled symbols) of 5 μM garcinol for 3 days.* ***(c)*** *Western blot analysis of whole-protein extracts of control and 3 day acetate-exposed OT-I memory T cells probed for acetylated-lysine. Left panel: representative blot; right panel: pooled data (Ctr, black dots; Ac, blue triangles). Bands were quantified and normalized to Actin and fold-change over control OT-I memory T cells determined.* ***(d)*** *GAPDH was immunoprecipitated in control and OT-I memory T cells exposed to acetate for 3 d, each. The figure represents detection of an acetylated peptide (K217) (green) in GAPDH among acetate-exposed but not control OT-I memory T cells. Yellow indicates coverage.* ***(e)*** *GAPDH activity in mouse fibroblasts transfected with wild-type (blue triangles) or K→A 217 mutated (black dots) GAPDH for 48–96 h. To test for overall acetylation-dependency of GAPDH activity, we treated cell lysates with the bacterial de-acetylase CobB (open symbols) or buffer control (filled symbols) for 1 h. Each dot represents data obtained from cells isolated from one mouse, bars indicate means of pooled data. One-way ANOVA (b) and (e), unpaired t test (a, protein), and Wilcoxon matched-pairs signed rank test (a, mRNA) and (c) were used to compare groups. **P < 0.01, ****P < 0.0001, ns = not significant.*

Lastly, building on these detailed molecular data we also investigated how T cell memory function related to the acetate-driven augmentation of GAPDH and the overall glycolytic activity in these cells. Both *in vitro* and *in vivo* acetate-augmented memory T cells were functionally superior to acetate-deprived counterparts (data not shown). A summary of the findings in this report are provided below **(Figure 9)** (42).

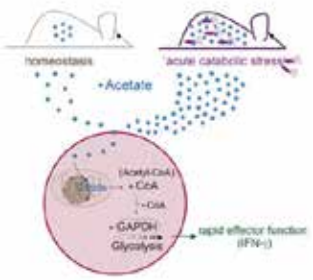

Figure 9. Graphical summary of how the organismal acute-phase acetate response is integrated at the cellular level in memory CD8⁺ T cells (from (42).

A path to clinical translation

Similar to acetate, also magnesium (Mg^{2+}) is an understudied component of the extracellular environment. Low dietary Mg^{2+} intake and hypomagnesemia have been implicated in the pathophysiology of various diseases, including infection and cancer (43–46). Only limited experimental data are available exploring how organismal Mg^{2+} abundance may affect the immune system. We recently found that the co-stimulatory cell-surface molecule LFA-1 requires Mg^{2+} to adopt its active conformation on $CD8^+$ T cells, thereby augmenting calcium flux, signal transduction, metabolic reprogramming, immune synapse formation and, as a consequence, specific cytotoxicity. Accordingly, magnesium-sufficiency sensed via LFA-1 translated to the superior performance of pathogen- and tumor-specific T cells and improved CAR T cell function (47) **(Figure 10):**

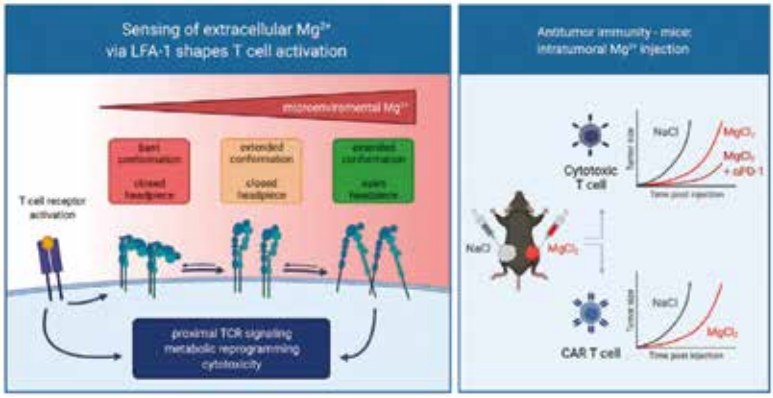

Figure 10. Graphical summary: mechanism of Mg^{2+} sensing by $CD8^+$ T cells and functional relevance of Mg^{2+} sufficiency (from (47).

This prompted us to retrospectively assess the relationship between serum Mg^{2+} levels and clinical outcomes in a CAR T cell trial and in an immune checkpoint inhibitor study. The CAR trial included a cohort of 100 patients with refractory B cell lymphoma treated with CD19-directed CAR T cells (Axicabtagene Ciloleucel), of which four had to be excluded from the retrospective analysis due to incomplete Mg^{2+}-serum testing. Patients were classified into two strata according to the mean Mg^{2+} level between days −5 and +3 of treatment (n = 5 measurements available for each patient). An arbitrary cut-off was set at 1.7 mg dl−1 for assigning patients into normo- versus hypomagnesemia groups **(Figure 11a,** *left panel*). Baseline characteristics of these retrospectively assigned study populations were similar, including age, ECOG performance status, and disease stage (data not shown). Although the number of patients with a mean Mg^{2+} level of <1.7 mg dl−1 was low, overall survival and median progression-free survival for these patients were reduced as compared with patients with normal serum Mg^{2+} levels **(Figure 11a,** *right panel*). We next explored how organismal Mg^{2+} abundance was associated with outcome in a cohort of non-small cell lung cancer (NSCLC) patients enrolled in an immune checkpoint inhibitor trial (SAKK16/14) (48). From a total of 67 initially

enrolled patients, two had to be excluded, leaving 65 that were treated with an anti-PD-L1 mAb (Durvalumab) in addition to neoadjuvant chemotherapy. Any detection of hypomagnesemia during the course of the trial assigned an individual to the hypomagnesemia group. This stratification strategy well discriminated the mean Mg^{2+} levels across all available measurements **(Figure 11b,** *left panel*). Also in this clinical trial, baseline characteristics were similar between the two retrospectively assigned groups (data not shown). Pathological complete response and overall survival **(Figure 11b,** *middle and right panels*), as well as radiographic response and event-free survival (data not shown) were all reduced in patients with hypomagnesemia. While these retrospective analyses have many limitations, in the context of our experimental data, the findings aligned with the concept that Mg^{2+}, by increasing LFA-1 outside-in signaling activity, may contribute to the clinical efficacy of CAR T cells and endogenous cancer-directed T cells in human patients. A prospective clinical trial is now being conducted.

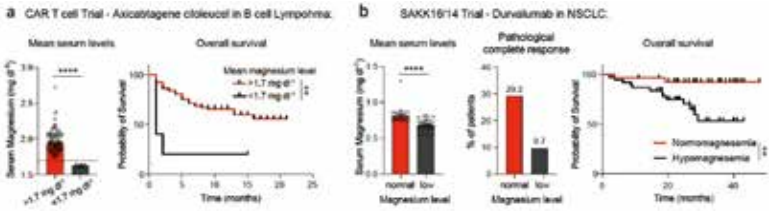

Figure 11. Serum magnesium levels and outcome in patients with cancer. (a) *Stratification of patients according to mean serum magnesium levels > 1.7 mg dl^{-1} versus <1.7 mg dl^{-1} between day −5 and day +3 of adoptive cell therapy, n = 5 measurements per patient (left panel). Each symbol represents one individual. Overall survival of patients stratified according to normal and low Mg^{2+} levels (right panel).* ***(b)*** *Comparison of mean serum magnesium levels after stratification according to occurrence of ≥1 hypomagnesemia-measurement during the trial (left panel). Complete pathological response (middle panel), and overall survival (right panel) according to this stratification. NSCLC, non-small cell lung cancer. Data are presented as median ± 95% CI left panel of (L and M). Statistical significance was assessed by unpaired Student's t test left panel of (a) and (b), and log-rank Mantel-Cox test in right panels of (a) and (b). **P < 0.01, **** P < 0.0001.*

Acknowledgments

First, I would like to express my gratefulness for having been selected to receive this prestigious award given out by the Prof. Dr. Max Cloëtta Foundation. It is important, however, to stress that I merely accept the award in the name of many. Specifically my many bright and hard-working colleagues that made all the discoveries with me over the years. There is no such thing as «my success» – it's our success, always. My deepest gratitude therefore goes to all my former and current lab members. Thank you: it has been, and is, an honor working with you – what a diverse group of driven, intelligent and original people you are!

I would further like to thank my mentors, Juerg Schifferli and Andrew Luster. Both trusted in me, allowed me to explore and taught me that biology is not organized in boxes.

A big thank you also goes to the Department of Biomedicine (DBM), my scientific home-base for many years. The excellent research environment and support provided by the DBM catalyzes creativity and enables efficient implementation of ideas.

The work done over the past many years was generously supported by numerous funding sources. Foremost the Swiss National Science Foundation, who supported my first project grant based on a rather sketchy (to say the least) preliminary set of data (which, however, turned out to be the very foundation of our research). Further funding was received from the Swiss Cancer League, Gebert Rüf Foundation, Botnar Foundation, Novartis Foundation and Uniscientia Foundation.

And while Science is undoubtedly fun, it would be void if I could not share my enthusiasm with my family, my parents and friends – and our dog, of course (such a great listener). When telling my wife, Viviane, and my children, Philippe, Aline, Dana and Oliver how we (again) solved all the world's problems, their loving twitting is the best way to end a day.

References

1. Suarez-Fueyo, A., Bradley, S. J., Tsokos, G. C. T cells in systemic lupus erythematosus. *Curr. Opin. Immunol.* **43,** 32–38 (2016)

2. Speiser, D. E., Ho, P. C., Verdeil, G. Regulatory circuits of T cell function in cancer. *Nat. Rev. Immunol.* **16,** 599–611 (2016)

3. McInnes, I. B., Schett, G. The pathogenesis of rheumatoid arthritis. *N. Engl. J. Med.* **365,** 2205–2219 (2011)

4. Wherry, E. J., Kurachi, M. Molecular and cellular insights into T cell exhaustion. *Nat. Rev. Immunol.* **15,** 486–499 (2015)

5. Sell, H., Habich, C., Eckel, J. Adaptive immunity in obesity and insulin resistance. *Nat. Rev. Endocrinol.* **8,** 709–716 (2012)

6. Bantug G.R., Galluzzi L., Kroemer G., Hess C. The spectrum of T cell metabolism in health and disease. *Nat. Rev. Immunol.* **18,** 19–34 (2018)

7. Haring, J.S., Badovinac, V.P., Harty, J.T. Inflaming the $CD8^+$ T cell response. *Immunity* **25,** 19–29 (2006)

8. Kaech, S.M., Wherry, E.J. Heterogeneity and cell-fate decisions in effector and memory $CD8^+$ T cell differentiation during viral infection. *Immunity* **27,** 393–405 (2007)

9. Fox, C.J., Hammerman, P.S., Thompson, C.B. Fuel feeds function: energy metabolism and the T-cell response. *Nat. Rev. Immunol.* **5,** 844–852 (2005)

10. Plas, D.R., Rathmell, J.C., Thompson, C.B. Homeostatic control of lymphocyte survival: potential origins and implications. *Nat. Immunol.* **3,** 515–521 (2002)

11. Frauwirth, K.A., Thompson, C.B. Regulation of T lymphocyte metabolism. *J. Immunol.* **172,** 4661–4665 (2004)

12. Frauwirth, K.A. et al. The CD28 signaling pathway regulates glucose metabolism. *Immunity* **16,** 769–777 (2002)

13. Jacobs, S.R. et al. Glucose uptake is limiting in T cell activation and requires CD28-mediated Akt-dependent and independent pathways. *J. Immunol.* **180,** 4476–4486 (2008)

14. Greiner, E.F., Guppy, M., Brand, K. Glucose is essential for proliferation and the glycolytic enzyme induction that provokes a transition to glycolytic energy production. J. Biol. *Chem.* **269,** 31484–31490 (1994)

15. Maciver, N.J. et al. Glucose metabolism in lymphocytes is a regulated process with significant effects on immune cell function and survival. *J. Leukoc. Biol.* **84,** 949–957 (2008)

16. Board, M., Humm, S., Newsholme, E.A. Maximum activities of key enzymes of glycolysis, glutaminolysis, pentose phosphate pathway and tricarboxylic acid cycle in normal, neoplastic and suppressed cells. *Biochem. J.* **265,** 503–509 (1990)

17. Wang, R. et al. The transcription factor Myc controls metabolic reprogramming upon T lymphocyte activation. *Immunity* **35,** 871–882 (2011)

18. Lunt, S.Y., Vander Heiden, M.G. Aerobic glycolysis: meeting the metabolic requirements of cell proliferation. *Annu. Rev. Cell Dev. Biol.* **27,** 441–464 (2011)

19. Masopust, D., Picker, L.J. Hidden memories: frontline memory T cells and early pathogen interception. *J. Immunol.* **188,** 5811–5817 (2012)

20. Geginat, J., Lanzavecchia, A., Sallusto, F. Proliferation and differentiation potential of human $CD8^+$ memory T-cell subsets in response to antigen or homeostatic cytokines. *Blood* **101,** 4260–4266 (2003)

21. Klonowski, K.D. et al. Dynamics of blood-borne CD8 memory T cell migration *in vivo.* *Immunity* **20,** 551–562 (2004)

22. Masopust, D., Vezys, V., Marzo, A.L., Lefrancois, L. Preferential localization of effector memory cells in nonlymphoid tissue. *Science* **291,** 2413–2417 (2001)

23. Sathaliyawala, T. et al. Distribution and compartmentalization of human circulating and tissue-resident memory T cell subsets. *Immunity* **38,** 187–197 (2013)

24. Kong, S., McBurney, M.W., Fang, D. Sirtuin 1 in immune regulation and autoimmunity. Immunol. *Cell Biol.* **90,** 6–13 (2012)

25. Fann, M. *et al.* Histone acetylation is associated with differential gene expression in the rapid and robust memory CD8⁺ T-cell response. *Blood* **108,** 3363–3370 (2006)

26. Juelich, T. *et al.* Interplay between chromatin remodeling and epigenetic changes during lineage-specific commitment to granzyme B expression. *J. Immunol.* **183,** 7063–7072 (2009)

27. Zediak, V.P., Johnnidis, J.B., Wherry, E.J., Berger, S.L. Cutting edge: persistently open chromatin at effector gene loci in resting memory CD8⁺ T cells independent of transcriptional status. *J. Immunol.* **186,** 2705–2709 (2011)

28. Wellen, K.E. et al. ATP-citrate lyase links cellular metabolism to histone acetylation. *Science* **324,** 1076–1080 (2009)

29. Gubser P.M., Bantug G.R., Razik L., Fischer M., Dimeloe S., Hoenger G., Durovic B., Jauch A., Hess C. Rapid effector function of memory CD8⁺ T cells requires an immediate-early glycolytic switch. *Nat. Immunol.* **14,** 1064–1072 (2013)

30. Theurey P., Rieusset J. Mitochondria-Associated Membranes Response to Nutrient Availability and Role in Metabolic Diseases. *Trends Endocrinol. Metab.* **28,** 32–45 (2017)

31. Murley A., Nunnari J. The Emerging Network of Mitochondria-Organelle Contacts. *Mol. Cell* **61,** 648–653 (2017)

32. Tubbs E., et al. Mitochondria-associated endoplasmic reticulum membrane (MAM) integrity is required for insulin signaling and is implicated in hepatic insulin resistance. *Diabetes* **63,** 3279–3294 (2014)

33. Bantug G.R., *et al.* Mitochondria-Endoplasmic Reticulum Contact Sites Function as Immunometabolic Hubs that Orchestrate the Rapid Recall Response of Memory CD8⁺ T Cells. Immunity **48,** 542–555 (2018)

34. Knowles S.E., Jarrett I.G., Filsell O.H., Ballard F.J. Production and utilization of acetate in mammals. *Biochem. J.* **142,** 401–411 (1974)

35. Beisel W.R., Metabolic response to infection. *Annu. Rev. Med.* **26,** 9–20 (1975)

36. Guan K.-L., Xiong Y. Regulation of intermediary metabolism by protein acetylation. *Trends Biochem. Sci.* **36,** 108–116 (2011)

37. Shestov A.A., et al. Quantitative determinants of aerobic glycolysis identify flux through the enzyme GAPDH as a limiting step. *eLife* **3** (2014)

38. Wiśniewski J.R., Gizak A., Rakus D. Integrating Proteomics and Enzyme Kinetics Reveals Tissue-Specific Types of the Glycolytic and Gluconeogenic Pathways. *J. Proteome Res.* **14,** 3263–3273 (2015)

39. Li T., et al. Glyceraldehyde-3-phosphate dehydrogenase is activated by lysine 254 acetylation in response to glucose signal. *J. Biol. Chem.* **289,** 3775–3785 (2014)

40. Balasubramanyam K., Altaf M., Varier R.A., Swaminathan V., Ravindran A., Sadhale P.P., Kundu T.K. Polyisoprenylated benzophenone, garcinol, a natural histone acetyltransferase inhibitor, represses chromatin transcription and alters global gene expression. *J. Biol. Chem.* **279,** 33716–33726 (2004)

41. Simon G.M., Cheng J., Gordon J.I. Quantitative assessment of the impact of the gut microbiota on lysine epsilon-acetylation of host proteins using gnotobiotic mice. *Proc. Natl. Acad. Sci. USA* **109,** 11133–11138 (2012)

42. Balmer M.L., *et al.* Memory CD8(+) T cells require increased concentrations of acetate induced by stress for optimal function. *Immunity* **44,** 1312–1324 (2016)

43. Costello R.B., Nielsen F. Interpreting magnesium status to enhance clinical care: Key indicators. *Curr. Opin. Clin. Nutr. Metab. Care* **20,** 504–511 (2017)

44. Larsson S.C., Orsini N., Wolk A. Dietary magnesium intake and risk of stroke: A meta-analysis of prospective studies. *Am. J. Clin. Nutr.* **95,** 362–366 (2012)

45. Ravell J., et al. Plasma magnesium is inversely associated with Epstein-Barr virus load in peripheral blood and Burkitt lymphoma in Uganda. *Cancer Epidemiol.* **52,** 70–74 (2018)

46. Sojka J.E., Weaver C.M. Magnesium supplementation and osteoporosis. *Nutr. Rev.* **53,** 71–74 (1995)

47. Lötscher J., et al. Magnesium sensing via LFA-1 regulates $CD8^+$ T cell effector function. *Cell* **185,** 585–602 (2022)

48. Rothschild S.I., *et al.* SAKK 16/14: durvalumab in addition to neoadjuvant chemotherapy in patients with stage IIIA(N2) non-small-cell lung cancer-a multicenter single-arm phase II trial. *J. Clin. Oncol.* **39,** 2872–2880 (2021)